

## Characterization of Voxel-Based Variance in DTI Measurements

D. M. Levy<sup>1</sup>, T. G. Fisher<sup>2</sup>, M. Chung<sup>3</sup>, J. E. Lee<sup>2</sup>, J. H. Lee<sup>4</sup>, M. Lazar<sup>1</sup>, T. R. Oakes<sup>1</sup>, J. S. Kim<sup>5</sup>, A. L. Alexander<sup>2</sup>

<sup>1</sup>Waisman Laboratory for Brain Imaging and Behavior, University of Wisconsin-Madison, Madison, WI, United States, <sup>2</sup>Medical Physics, University of Wisconsin-Madison, Madison, WI, United States, <sup>3</sup>Statistics, University of Wisconsin-Madison, Madison, WI, United States, <sup>4</sup>Biomedical Engineering, University of Wisconsin-Madison, Madison, WI, United States, <sup>5</sup>Radiology, University of Wisconsin-Madison, Madison, WI, United States

### Introduction:

Voxel-based statistical analysis methods have recently been applied in a broad range of DTI applications to investigate between-group comparisons and correlations with external measures. These studies most commonly use maps of the fractional anisotropy (FA), although several studies have also used maps of the average apparent diffusion coefficient (ADC). The design and interpretation of these results is highly dependent upon the sources of variance in these images. In this study, a voxel based analysis was used to characterize different sources of variance (acquisition-dependent and between-subject) in DTI data from a young adolescent cohort.

### Methods:

**Imaging Protocol:** DTI studies were performed on fourteen healthy early adolescent subjects (ages 11-12, 7M:7F) using a 3.0T GE SIGNA MRI scanner. The imaging was repeated on 3 separate days within 6 weeks to estimate the variance of DTI measurements within single subjects. The DTI protocol parameters were quad birdcage head coil, cardiac-gated (13 R-R) single-shot DW EPI, 39 contiguous 3 mm thick axial slices covering the cerebrum, 12 uniform encoding directions, diffusion-weighting = 1114 s/mm<sup>2</sup>, 240 mm FOV, 120x120 matrix, and 3 NEX. The total acquisition time was roughly 6-9 minutes dependent upon the subjects heartrate. Distortions from eddy currents and B0 inhomogeneities were corrected using a 2D affine image registration program (AIR - /bishopw.loni.ucla.edu/AIR5/), and a custom field map correction method. 3D maps of FA and ADC were subsequently calculated from the corrected DTI data.

**Within-Subject Variance (WSV):** The set of three FA and ADC maps for each subject were co-registered using an image co-registration program (flirt - FSL - www.fmrib.ox.ac.uk/fsl/). For each subject, voxelwise maps of within-subject mean FA (mFA<sub>i</sub>), mean ADC (mADC<sub>i</sub>), FA variance (vFA<sub>i</sub>), and ADC variance (vADC<sub>i</sub>) were calculated. The data sets from each subject were then spatially normalized to a template FA image using a 3D affine image registration algorithm in flirt. The vFA<sub>i</sub> and vADC<sub>i</sub> maps were averaged across subjects to create voxel-based maps of mean within-subject FA variance ( $\sigma_{\text{FA}}^2$ ) and ADC variance ( $\sigma_{\text{ADC}}^2$ ). The mean within-subject variance measures represent the variations that predominately arise from the acquisition (system stability, noise & artifacts), image processing (artifact correction), and physiological differences within the subject. Image calculations were performed using SPAMALIZE software (/brainimaging.waisman.wisc.edu/~oakes/spam/spam\_frames.htm).

### Between-Subject Variance (BSV):

The spatially normalized mFA<sub>i</sub> and mADC<sub>i</sub> for each subject were averaged to calculate overall (between-subject) 3D maps of mean FA (<FA>) and mean ADC (<ADC>) maps, and the between-subject FA variance ( $\sigma_{\text{FA}}^2$ ) and ADC variance ( $\sigma_{\text{ADC}}^2$ ) were also calculated on a voxelwise basis. The between-subject variance measures represent a combination of the underlying differences in FA and ADC between subjects as well as image registration error.

### Results & Discussion:

Maps of the between subject-mean, square root of the BSV, and square root of the mean WSV are shown in the Figure. These maps demonstrate that the WSV are generally lower than the BSV for both FA and ADC in this data set. The ADC variance maps are generally higher in regions of CSF and brainstem. The BSV of FA is highest in areas around the corpus callosum and in subcortical white matter, which is most likely from errors in affine image registration. This source of variance is expected to decrease with improved (e.g., non-rigid) image co-registration algorithms. The WSV of FA shows hyperintense regions in ventral temporal lobe and OFC areas that are most affected by B0 inhomogeneities, which are most likely to vary between imaging sessions. Voxel-based statistical analyses (e.g., SPM) will be less sensitive in regions with greater WSV or BSV. The characterization of WSV is critical for the sensitivity of longitudinal study designs. Further, measurements of WSV and BSV would be valuable for estimating statistical power and determining necessary sample sizes for study design. The formalism outlined here could be used to investigate the changes in variance with different image registration algorithms. Although not done in this study, the repeated measurements in the same subjects also allow for the unique opportunity to construct mean images weighted by the variance estimated for each subject.

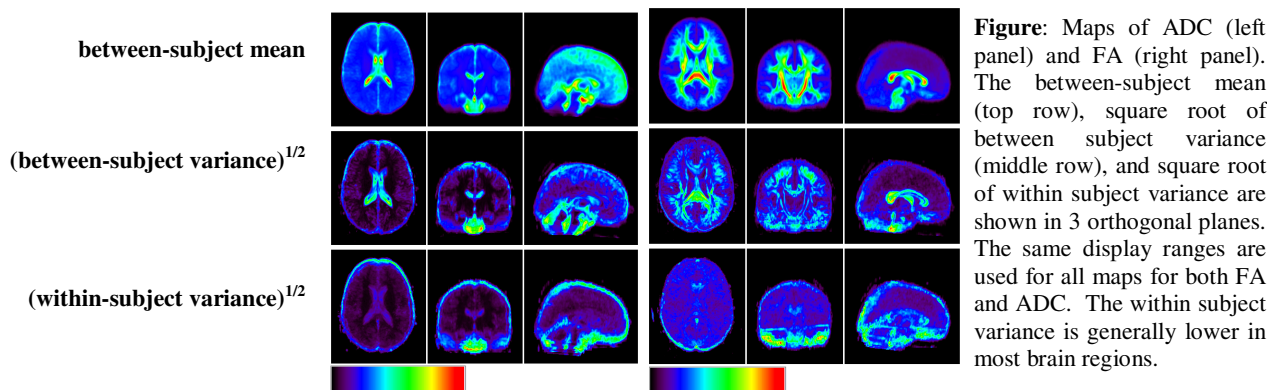


**Figure:** Maps of ADC (left panel) and FA (right panel). The between-subject mean (top row), square root of between subject variance (middle row), and square root of within subject variance are shown in 3 orthogonal planes. The same display ranges are used for all maps for both FA and ADC. The within subject variance is generally lower in most brain regions.